Effect of pulse duration on resonant heating of laser-irradiated argon and deuterium clusters

Ayush Gupta and T. M. Antonsen
Department of Electrical Engineering, University of Maryland, College Park, Maryland 20770 and Institute for Research in Electronics and Applied Physics, University of Maryland, College Park, Maryland 20770, USA

T. Taguchi
Department of Electrical and Electronics Engineering, Setsunan University, Neyagawa, Osaka, Japan

J. Palastro
Department of Physics, University of Maryland, College Park, Maryland 20770, USA and Institute for Research in Electronics and Applied Physics, University of Maryland, College Park, Maryland 20770, USA

(Received 29 June 2006; revised manuscript received 16 August 2006; published 25 October 2006)

We study the effect of pulse duration on the heating of single van der Waals bound argon and deuterium clusters by a strong laser field using a two-dimensional (2D) electrostatic particle-in-cell (PIC) code in the range of laser-cluster parameters such that kinetic as well as hydrodynamic effects are active. Heating is dominated by a collisionless resonant absorption process that involves energetic electrons transiting through the cluster. A size-dependent intensity threshold defines the onset of this resonance [T. Taguchi *et al.*, Physical Review Letters, **92**, 20 (2004)]. It is seen that increasing the laser pulse duration lowers this intensity threshold and the energetic electrons take multiple laser periods to transit the cluster instead of one laser period. Our simulations also show that strong electron heating is accompanied by the generation of a high-energy peak in the ion energy distribution function. We also calculate the yield of thermonuclear fusion neutrons from exploding deuterium clusters using the PIC model with periodic boundary conditions that allows for the interaction of ions from neighboring clusters.

DOI: 10.1103/PhysRevE.74.046408 PACS number(s): 52.50.Jm, 36.40.Gk, 52.38.Kd, 52.38.Dx

I. INTRODUCTION

Clusters are nanoscale solid density atomic aggregates bound by van der Waals forces ranging in size from 10^2 – 10^6 atoms. Clusters are formed when high-pressure flow of a cooled gas into vacuum results in adiabatic cooling and expansion of the gas and particle aggregation [1]. The volume average density of clustered gases is low but the clusters themselves are at solid density. This enables strong interaction of individual clusters with an irradiating laser pulse while still allowing propagation of the pulse through the clustered gas. The efficient coupling of laser energy into clustered gases [2] makes them a unique media for studying nonlinear laser-matter interaction [3] and leads to many exciting applications. The laser-heated clusters generate x-ray and extreme ultraviolet (EUV) radiation, and high-energy ions and electrons [4,5]. Collisions between energetic ions from exploding clusters can produce neutrons via thermonuclear fusion [5,6]. The dynamics of exploding clusters gives rise to interesting nonlinear optical effects such as harmonic generation [7] and self-focusing [8]. Clustered gases are also proposed as targets for creating plasma wave guides [9].

The interaction of clusters with strong laser fields is characterized by a large number of tunable parameters such as the peak intensity, pulse duration, spot size, frequency and field polarization of the laser pulse, the distribution of cluster sizes, fraction of gas present as monomers, and the density and ionization potentials of the cluster atoms. Various experimental [10–13] and theoretical studies [14–19] have explored the role played by some of these parameters with theoretical studies often focused on the effect of laser intensity and cluster size. Experimental studies show that pulse duration plays an important role in the various aspects of laser-cluster interaction such as absorption and scattering of laser pulses [20], neutron yield of deuterium cluster targets [12], x-ray generation [13], and extreme ultraviolet emission [13,21]. In the present work we examine via simulations the effect of laser pulse duration [full width at half maximum (FWHM) of the laser pulse envelope] on heating of irradiated argon and deuterium clusters. We also examine the yield of fusion neutrons from exploding deuterium clusters for a range of intensities.

The manner in which individual clusters are heated by the laser pulse and explode has several characteristic regimes based on the laser intensity and size of cluster. Two relatively distinct regimes are hydrodynamic expansion and Coulomb explosion. For high intensities or small clusters most electrons are removed from the cluster early in the pulse and the cluster "Coulomb explodes" due to the repulsion of the remaining positive ions. Typically [22] particle models have been used to study this regime. In these models the electrostatic interaction between particles is treated point wise (particle to particle, also known as molecular dynamics simulations) or in the particle in cell (PIC) approximation. The molecular dynamics method is suited for small clusters and becomes computationally inefficient for large clusters. The PIC method is more practical for large clusters. It is, however, relatively more difficult to describe collisions in the PIC framework.

At lower intensities and for large clusters a hydrodynamic approach is valid. Here, the expansion is driven by the pressure of electrons. In this approach, the cluster is modeled using fluid equations. The first study of hydrodynamic ex-

pansion of clusters [23] treated the ionized clusters as a spherical ball of uniform "nanoplasma" with no density or temperature gradients. The electrons are generated by field and collisional ionization and heated primarily by the electron-ion collisions within the cluster. For the brief time interval when the electron plasma frequency in the expanding cluster satisfies $\omega_{p0}=\sqrt{3}\ \omega_0$, where ω_0 is the laser frequency, an electrostatic resonance causes the field inside the cluster to rise sharply leading to rapid heating. A more sophisticated approach allows for nonuniformity of temperature and density during expansion [16]. This model predicts that the dominant energy absorption occurs in regions where the electron density is near the critical density. The main consequence of this is that strong absorption occurs over a much longer duration than that predicted by the uniform density model. In both these models, the response of the cluster to the laser electric field is treated in the cold plasma approximation and is used for calculation of the total electric field as well as the energy absorbed by the cluster. However, when energetic particles are produced the local cold plasma approximation no longer applies. Energetic particles travel a distance comparable to the cluster size in a laser period contributing to a nonlocal and nonlinear dielectric response. This necessitates a kinetic treatment of the absorption process.

Our studies have used a PIC model focused on this intermediate range of intensity and cluster sizes where a population of energetic electrons is produced and the heating and expansion of the cluster are distinctly nonhydrodynamic. However, the cluster still remains quasineutral as it expands. In this regime energy absorption by electrons is both a kinetic and a collective effect. The energetic electrons make large excursions, comparable to the size of the cluster, and being at a high temperature are largely unaffected by collisions (refer to the fact that collision frequency is inversely proportional to temperature). At the same time, the laser field is strongly shielded from the cluster core by the dielectric response of the electrons. Other similar particle studies have not considered ion motion [24] which significantly affects the cluster expansion dynamics for long pulse, or do not work in the regime of free electron excursion comparable to the cluster diameter for several laser periods [14] which is our regime of interest.

The major result of our previous studies [17,18] was that there is a well defined intensity threshold above which energetic electrons are created by an absorption process related to that proposed by Brunel for sharp density gradients [25]. Electrons are first accelerated out from the cluster and then driven back into it by the combined effects of the laser field and the electrostatic field produced by the laser-driven charge separation. The energetic electrons then pass through the cluster and emerge on the other side. If they emerge in phase with the laser field, there is resonant heating, and the cluster quickly absorbs energy. The onset of this resonance corresponds to the intensity for which the excursion of a free electron in the laser field is comparable to the cluster diameter. This critical intensity was shown to be

$$I_0 = \frac{c}{8\pi}\left(\frac{m_e\omega^2}{2\pi e}\right)^2 D^2{}_0, \tag{1}$$

where c is the speed of light in vacuum, D_0 is the initial cluster diameter, ω is the frequency of the laser pulse, and m_e and e are the electron mass and charge, respectively.

In this paper, we use our PIC model to examine how laser pulse duration influences the energy absorption by clusters. Our simulations show that increasing the pulse duration enables strong heating via a higher order electron transit time resonance where the electron transit time through the cluster equals multiple laser periods, effectively lowering the intensity threshold for strong heating. We modify the scaling law for the intensity threshold derived in Ref. [17] to take the higher order electron transit time resonance into account.

Fusion of ions from exploding deuterium clusters as observed in experiments has generated interest in laser irradiated clustered gases as a potential source of fusion neutrons. Some past studies [11,12,14,19,26] have investigated fusion neutron yield in the Coulomb explosion regime. In the present work, we use the ion energy spectrum from our PIC model to estimate the fusion yield from deuterium clusters for a range of pulse intensities and examine the effect of intensity threshold on fusion yield in the regime where both kinetic and hydrodynamic effects are active.

The organization of the paper is as follows. The simulation model used is described in Sec. II. Simulation results showing the effect of nonlinear resonance on heating of argon and deuterium clusters for a range of intensities at different pulse durations are outlined in Sec. III. Modification to the scaling law for strong heating to incorporate the effects of increased pulse width is included in this section. Section IV presents the electron and ion distribution functions for argon and deuterium clusters. The deuterium ion energy spectrum is used in Sec. V to estimate the fusion yield for a range of pulse intensities. Section VI ends the paper with discussions and concluding remarks.

II. PIC MODEL OF CLUSTER EXPANSION

To study the effect of laser pulse parameters on cluster heating in the transition regime, we use a two-dimensional (2D) electrostatic particle-in-cell (PIC) model which has been presented in detail in Refs. [17,18]. The laser field $E=E_x(t)\sin\omega t$ is polarized in the x direction with frequency ω corresponding to $\lambda=800$ nm, and time dependent amplitude $E_x(t)$ corresponding to a Gaussian pulse. The electrostatic calculation is appropriate in the near field limit ($D_0/\lambda \ll 1$), and for intensities below $\sim 5\times 10^{17}$ W/cm^2. For higher intensities, where the quiver velocity approaches the speed of light, the Lorentz force becomes important, necessitating an electromagnetic simulation.

As the intensity rises past a threshold ($\sim 10^{14}$ W/cm^2 for argon atoms) during the pulse neutral cluster atoms are ionized by field ionization followed by collisional ionization. This produces a supercritically dense plasma with electron density $n_e > n_{cr}$, where n_{cr} is the density at which the electron plasma frequency equals the incident laser frequency. The plasma shields the core of the cluster from the laser field. The majority of our simulations begin here by modeling the clusters as consisting of preionized atoms and electrons. The material parameters used for argon and deuterium clusters are specified in Table I. The initial temperatures in either case are chosen to be 10 eV for electrons and 0 eV for ions.

TABLE I. Cluster parameters for argon and deuterium clusters.

Cluster amaterial	Initial ion density (cm^{-3})	Maximum ionized state, Z	Initial electron density	Mass of ion (amu)
Argon	1.742×10^{22}	$Z=8$	$n_e\sim80\ n_{cr}$	40
Deuterium	5.98×10^{22}	$Z=1$	$n_e\sim34\ n_{cr}$	2

This electron temperature is large enough to suppress grid instabilities inherent to PIC algorithm, but not so large as to affect results. Electron-ion scattering processes are included explicitly in our code through a Monte Carlo method, but ion-ion and electron-electron scattering processes are neglected. Over the few hundred femtoseconds of the simulation, collisional energy relaxation from electrons to ions is not important, and the ions gain energy dominantly through acceleration by the space-charge electric field.

The 2D simulations, corresponding to an initially cylindrical cluster, are carried out on a 1024×1024 square mesh of spacing 0.805 nm. In most of our simulations, unless otherwise stated, we solve the Poisson equation with open boundary conditions, and particles are allowed to leave the simulation region. Once a particle leaves, its momentum and position are still tracked assuming it responds only to the laser electric field. This is important in calculating the electric dipole moment of the exploding cluster. The distance to the simulation boundary is sufficiently far from the cluster core that only a small fraction of the electrons leave the simulation box for most of the pulse duration.

We note that three-dimensional (3D) simulations that we have carried out earlier and reported in Refs. [17,18] show the same behavior as found in the 2D simulations reported there [17,18] and here. The only difference is a lowering of the threshold intensity due to the increased dielectric focusing found in 3D geometry. Thus, for the extensive study of the effect of pulse duration we restrict ourselves to the less computationally intensive 2D simulations.

If the number density of clusters in the irradiated volume is high, energetic ions from neighboring clusters are expected to interact especially towards the end of the pulse when the cluster has expanded significantly. The effect of neighboring clusters alters the evolution of the energy spectrum of ions and electrons. The energy distribution of ions is directly used for determining the fusion neutron yield. In order to incorporate the effect of ions from neighboring clusters on the kinetic energy distribution of ions, we employ periodic boundary conditions to solve the Poisson equation and we allow escaping particles to reenter the simulation domain. In this case, the size of the simulation box defines the intercluster distance. We assume that the clusters are distributed uniformly in the irradiated volume. Then the intercluster distance is simply $(n_{cl})^{-1/3}$, where n_{cl} is the number density of clusters. For our simulations parameters (1024×1024 mesh with mesh spacing of 0.805 nm), the intercluster distance is 824.32 nm which corresponds to $n_{cl}=1.78\times10^{12}\ cm^{-3}$.

III. EFFECT OF PULSE DURATION

We have done a series of PIC simulations for a range of peak intensities at three different pulse widths for both Argon and Deuterium. The initial cluster radius was fixed at $D_0=38$ nm. The pulse width defined the full width at half maximum of the Gaussian laser pulse envelope. The peak intensity is varied from $1\times10^{13}\ W/cm^2$ to $1\times10^{16}\ W/cm^2$ with the pulse widths corresponding to FWHM of 100 fs, 250 fs, and 1 ps for argon and 70 fs, 100 fs, and 500 fs for deuterium.

In Fig. 1, we plot the average kinetic energy per electron for cluster electrons (solid) and ions (dotted), and the electrostatic field energy per electron (dashed) in the cluster for $D_0=38$ nm and laser peak intensity of $3\times10^{15}\ W/cm^2$ and pulse width of 250 fs. Also shown is the laser intensity profile. Initially, the laser electric field pulls out a small fraction of the electrons at the cluster boundary. Accelerated by the electric field in the cluster potential, these escaped electrons absorb energy and the mean electron kinetic energy is increased. As the laser intensity rises, more electrons are pulled out of the cluster and electron excursion length is also increased resulting in stronger heating of the cluster. The mechanism of electron heating is described in detail when we discuss phase space plots later in the paper. The charge imbalance created by the extraction of electrons causes an outward directed electric field that accelerates the ions. The electron energy is thus transferred to ions via the electrostatic field energy stored in the space-charge field. The cluster expands due to the Coulomb force of the space charge on the cluster ions. Electron extraction and heating decreases later in the pulse when the laser electric field starts falling and the cluster boundary has expanded. This, accompanied by the continued expansion of the cluster core, causes the electron and field energies to fall. Towards the end of the pulse the

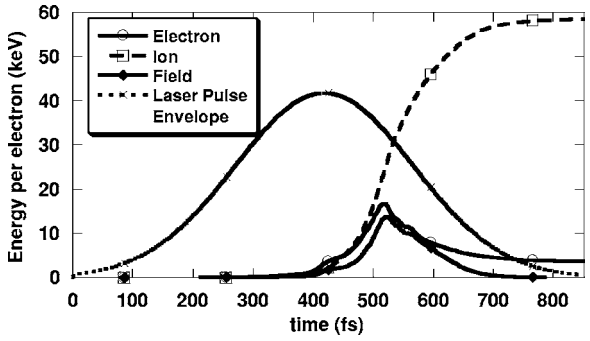

FIG. 1. Electron (solid line with circles), ion (dashed line with squares) and electrostatic field energy (solid line with diamonds) per cluster electron as a function of time for an argon cluster with $D_0=38$ nm and laser pulse of peak intensity $3\times10^{15}\ W/cm^2$ and FWHM of 250 fs. The laser field profile is shown on the same time axis by the dotted line with crosses. The applied field accelerates the electrons, creating a charge separation that in turn accelerates the ions.

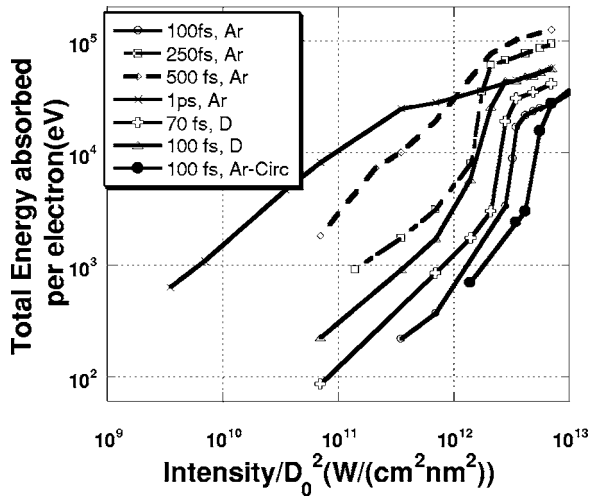

FIG. 2. Total energy absorbed by the cluster (sum of electron, ion and electrostatic field energies) per cluster electron versus the laser intensity for a range of pulse durations for argon and deuterium clusters. The curves are labeled in the legend by the pulse duration for that curve and as Ar for argon and D for deuterium. The curve labeled 100 fs, Ar-Circ is for a circularly polarized laser pulse of duration 100 fs. All other curves are for linearly polarized laser pulse. The laser intensity has been normalized to the square of the initial diameter of the cluster. Note the dramatic intensity threshold for strong energy absorption for both argon and deuterium at lower pulse durations. The intensity threshold is lowered as the pulse length is increased, and becomes less prominent for very long pulse lengths.

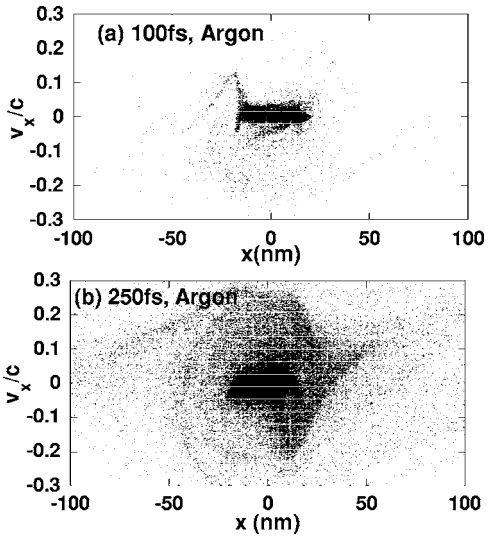

FIG. 3. Phase space $(x\text{-}v_x)$ plots for electrons near the x axis for Argon cluster. The two plots correspond to peak laser intensity and pulse length of (a) 5×10^{15} W/cm^2, 100 fs and (b) 5×10^{15} W/cm^2, 250 fs. Note that $N_{res}=1$ for (a) and $N_{res}=2$ for (b). Increase in the order of resonance leads to lowering of intensity threshold.

space charge field energy approaches zero as the expanding ions decrease the charge imbalance. The mean ion energy saturates as most of the electron energy is transferred to the ions and the electrons are no longer extracting energy from the pulse.

Our simulations indicate that there is an intensity threshold for strong heating at which there is a sharp increase in the laser energy coupled to the cluster electrons. This threshold effect is seen clearly in Fig. 2 that plots the total absorbed energy (sum of electron, ion, and electrostatic field energy) per electron at the end of the pulse versus peak laser intensity (scaled to the cluster diameter squared) for different pulse durations—100 fs, 250 fs, 500 fs, and 1 ps for argon (labeled as "Ar" in the legend) and 70 fs and 100 fs for deuterium (labeled with a "D" in the legend). The curves for shorter pulse durations (100 fs, 250 fs for argon and 70 fs, 100 fs for deuterium) exhibit a steep rise in the absorbed energy indicating that there is a critical intensity beyond which the cluster experiences enhanced heating. This threshold intensity is different for different cluster material (argon/deuterium) and laser pulse duration. In Ref. [17], it was shown for the case of 100 fs pulse duration and argon clusters that the threshold for strong absorption is due to a nonlinear electron transit time resonance. The critical intensity for the onset of this resonance was predicted as the intensity for which energetic electrons take exactly a laser period to transit once through the cluster. The dependence on cluster material and laser pulse duration as seen here is not predicted by the scaling law predicted by Taguchi *et al.* [17] and Antonsen *et al.* [18]. In the following paragraphs we will look at electron phase space plots to explore this in greater detail. The thresholdlike behavior is less prominent for the longer pulse duration of 500 fs and almost disappears for the even longer pulse width of 1 ps. The absence of a clear threshold for the 1 ps pulse duration results from strong heating of the cluster over a wider range of peak laser intensities and we look at electron phase space plots at three different intensities for 1 ps pulse duration to understand the process of laser to cluster energy for long pulse durations. Further, we note that in all cases the average energy absorbed per electron reaches a saturation value at high intensity, and that the saturation value does not depend monotonically on pulse duration. In particular, for argon cluster, the saturation value for pulse duration of 250 fs exceeds that for both 100 fs and 1 ps pulses. The curve labeled "Ar-Circ" is for a series of runs for argon clusters irradiated with circularly polarized laser light of 100 fs pulse duration.

The process of energy absorption by cluster electrons is related to that proposed by Brunel for heating of laser-driven electrons at planar solid-vacuum interface where the electron excursion amplitude is larger than the local density scale length. This is applicable to clusters where the laser pulse accelerates energetic electrons out from the cluster core and drives them back into the shielded cluster. We look at the electron phase space at peak laser intensity of 5×10^{15} W/cm^2, just beyond the threshold for the case of 100 fs pulse duration. Figure 3(a) shows a snapshot of this phase space at $t=188.17$ fs (the peak of the pulse occurs at 170 fs). Here, the axes are the x coordinate of position and the x component of velocity (v_x) for all electrons in the narrow layer $|y|<\Delta$ along the x axis, where Δ is the grid size. The high concentration of particles in a band about the center at small v_x represents the core electrons in the cluster. In this

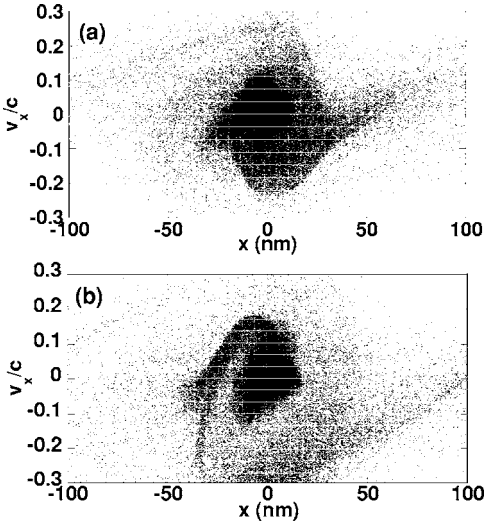

FIG. 4. Phase space (x-v_x) for electrons near the x axis for deuterium cluster for (a) 100 fs FWHM, 3×10^{15} W/cm^2 peak intensity at t=204.8 fs and (b) 70 fs FWHM, 5×10^{15} W/cm^2 peak intensity at t=148.9 fs. The plots show that N_{res}=2 for (a) and N_{res}=1 for (b).

region, the laser field is strongly shielded. We note that this core region is roughly 40 nm in size, indicating that the cluster does not expand appreciably before the time of this phase plot. The less dense bunch of electrons at higher magnitudes of velocity corresponds to energetic electrons in the range of 2–10 keV, which have been pulled out from a thin layer at the cluster surface by the laser electric field. The laser field accelerates these electrons and passing through the cluster they emerge on the other side in phase with the laser field and are further accelerated. The energetic electrons of Fig. 4 take one full laser period to travel once around the cluster to come back to the same position. This matching of electron transit time to the laser period sets up the resonance condition for irradiating laser pulse of 100 fs duration as described by Taguchi *et al.* [17] and Antonsen *et al.* [18].

Figure 3(b) plots the phase space for a laser pulse of 250 fs FWHM with peak intensity 3×10^{15} W/cm^2 at t =432.4 fs (the peak of the laser pulse occurs at 430.2 fs). As seen from Fig. 2, this corresponds to an intensity just beyond the threshold for strong heating and corresponds to 5×10^{15} W/cm^2 for the 100 fs pulse duration. Here, there are two tendrils of energetic electrons, and each bunch moves halfway around the cluster in a laser period. Thus the energetic electron transit time for 250 fs case equals twice the laser period.

Let the number of laser periods required by the hot electron bunch to transit once around the origin of the phase space be defined as N_{res}. Then N_{res}=1 for a 100 fs pulse, and N_{res}=2 for a 250 fs pulse. In the following paragraph we show that the electron transit time resonances with higher values of N_{res} would lead to a lower intensity threshold.

We assume that the cluster has not expanded appreciably before the onset of strong heating. Phase space plots of Fig. 3 show that this assumption holds reasonably well for those cases. For enhanced cluster heating characterized by an electron transit time resonance of order N_{res}, we can write the condition for strong heating as

$$\left(\frac{2D_0}{v_{cluster}}\right) = N_{res}\left(\frac{2\pi}{\omega}\right), \tag{2}$$

where D_0 is the initial cluster diameter, $v_{cluster}$ is the average velocity of an electron transiting the cluster, N_{res} is the order of resonance at the time of strong heating, and ω is frequency of the laser pulse. For the case of electron heating at a planar-solid interface considered by Brunel [25], the peak velocity of electrons driven into the planar surface was given as $v_{plane}=2eE_s/m_e\omega$, where E_s is the laser field at the surface, and the factor of 2 is due to the effective field boost provided by the space charge. The space charge field acts opposite the laser electric field during extraction, but adds to it when electrons are accelerated back into the bulk plasma. For our case of laser heating in clusters for the 2D geometry, there is an additional factor of 2 due to the dielectric focusing of the electric field lines by the cylindrical cluster. The extracted electrons, however, do not all have the same energy nor are they at the same phase with respect to the laser field resulting in the typical velocity of electrons transiting the cluster being lower than the peak velocity. We assume it to be half the peak velocity, i.e., $v_{cluster}=0.5(2v_{plane})=v_{plane}$. Substituting this in Eq. (2) we get the scaled critical intensity for strong absorption as

$$\frac{I_0}{D_0^2} = \frac{c}{8\pi}\left(\frac{m_e\omega^2}{2\pi e}\right)^2 \frac{1}{N_{res}^2}. \tag{3}$$

The threshold intensity is inversely proportional to the order of resonance as seen in Eq. (3). Thus the intensity threshold for 250 fs pulse duration (N_{res}=2) is lower than that for 100 fs case (N_{res}=1). It is important to note that the cluster does undergo higher N_{res} stages even for the case of 100 fs FWHM and peak intensity 5×10^{15} W/cm^2 earlier in the pulse [17], but the cluster does not absorb significant energy at these higher resonances. Because of the strong shielding effect of the core electrons, energetic electrons gain energy only when they are outside the cluster. The higher the order of the resonance, the smaller the fraction of time an electron is heated. Consequently, for strong absorption at higher N_{res} the cluster needs to spend longer time at the resonance. This is possible only with longer pulse durations where the temporal variation of the laser electric field is lower. For the 250 fs laser pulse, the cluster spends a significant time in a resonance stage characterized by N_{res}=2 and experiences enhanced laser pulse energy absorption at the lower peak intensity of 3×10^{15} W/cm^2. For 100 fs pulse width the laser pulse envelope varies more quickly and the peak laser intensity needs to be as high as 4.7×10^{15} W/cm^2 at which the cluster electrons gain energy with every laser cycle (N_{res}=1) and experience strong heating.

Figure 4 plots similar phase space plots for deuterium clusters for a laser pulse of (a) 100 fs FWHM, 3×10^{15} W/cm^2 peak intensity at t=204 fs, and (b) 70 fs FWHM, 5×10^{15} W/cm^2 peak intensity at t=148.9 fs. We note that for the 100 fs case, there are two bunches of energetic electrons indicating that N_{res}=2, while N_{res}=1 for the

70 fs case. The intensity threshold is accordingly lower for laser pulse width of 100 fs FWHM.

We see that the same threshold behavior is operative in both argon (atomic mass=40) clusters and deuterium (atomic mass=2) clusters. For short pulses the threshold is determined by the resonance condition with $N_{res}=1$ and for somewhat longer pulses with $N_{res}=2$. If we compare the two heating curves in Fig. 2 that correspond to $N_{res}=1$ resonance, viz. argon with pulse length 100 fs and deuterium with pulse length 70 fs, we see that they are quite similar, in spite of the factor of 20 difference in the ion mass. The same can be said of the two $N_{res}=2$ curves: Argon with pulse length 250 fs and deuterium with pulse length 100 fs. Thus, the main difference between argon and deuterium clusters is that the transition between $N_{res}=1$ and $N_{res}=2$ occurs for slightly larger pulse durations in the argon case than in the deuterium case. Our simulations seem to indicate that energy absorption by clusters is much more sensitive to changes in pulse duration rather than scaling of ion mass.

Another feature observed in Fig. 2 is the decreased prominence of the intensity threshold for longer laser pulse durations (500 fs and 1 ps runs). As the pulse duration is increased the manner of energy absorption by the cluster changes significantly. This is seen in Fig. 5 that plots (a) the total energy absorbed per cluster electron versus time and (b) root mean squared radius (RMS) of the cluster ions versus time for the peak laser intensities and pulse durations of (5×10^{15} W/cm^2, 100 fs), (3×10^{15} W/cm^2, 250 fs), and (5×10^{14} W/cm^2, 1 ps). These correspond to the intensities beyond which the total energy absorbed saturates for the particular pulse length. For the 100 fs and 250 fs pulse lengths these peak intensities are just above the threshold for strong heating. The plotted RMS radius of the cluster ions is normalized to the initial RMS value and is a measure of cluster expansion. In either figure, time (horizontal axis) is normalized to the pulse length. The shape of the pulse envelope is shown as the thin dotted line in Fig. 5(a). We note that for 100 and 250 fs cases energy absorption by the cluster takes place later in the pulse with fastest absorption taking place just after the peak has passed. This is due to enhanced heating with the onset of the transit time resonance. For the case of 1 ps pulse length, however, the cluster starts absorbing energy much earlier in the pulse when the intensity is low. In addition, Fig. 5(b) shows that the cluster starts expanding much earlier in the pulse for longer pulse lengths. Specifically the RMS radius of cluster ions increases to roughly 20 times the initial value for the case of 1 ps pulse length and to about 1.5 times the initial value for 250 fs, while it hardly changes for the shorted pulse length of 100 fs. In the following paragraph we look at electron phase space plots for the 1 ps case.

Figure 6(a) shows the phase space plot at t=1720 fs (peak of pulse is at 1700 fs) for a cluster irradiated with a laser pulse of 1 ps FWHM and peak intensity 5×10^{14} W/cm^2. In the phase space plot we can make out 9 distinct bunches of energetic electrons. In other words, $N_{res}=9$ for the conditions of Fig. 6(a). In addition, we note that the cluster core is significantly enlarged. This is because the cluster absorbed energy and expanded earlier in the pulse when the intensity was lower. In Figs. 6(b) and 6(c), we look at phase space

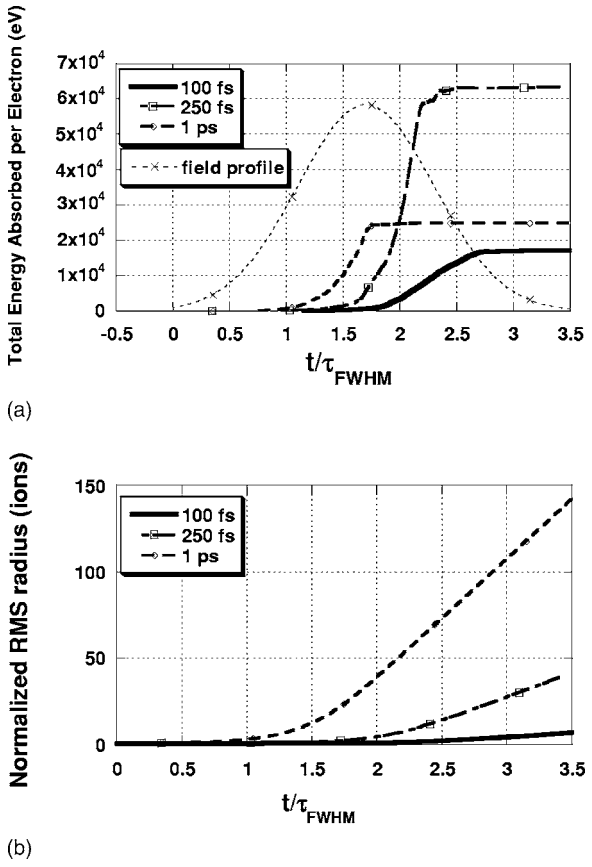

FIG. 5. (a) Total energy absorbed per electron and (b) Root mean squared radius of cluster ions for 100 fs, 5×10^{15} W/cm^2 (solid), 250 fs, 3×10^{15} W/cm^2 (dashed), and 1000 fs, 5×10^{14} W/cm^2 (dash-dot). For the case of 1 ps pulse length, the cluster absorbs energy and expands much earlier in the pulse when the electric field is much below the peak.

plots at lower peak intensities 1×10^{14} W/cm^2 (7b) and 5×10^{13} W/cm^2 (7c). The basic characteristics of these phase spaces are similar to the higher intensity case of 5×10^{14} W/cm^2 but show even higher orders of resonances of $N_{res}=10$, and $N_{res}=16$, respectively. The phase space study shows that at pulse length of 1 ps, the cluster can spend much longer times at each resonance stage leading to significant energy absorption at very high orders of resonance and lower peak intensities. As the peak intensity increases it supports lower orders of resonance and absorbs energy more efficiently, finally leading to saturation in energy absorbed beyond 5×10^{14} W/cm^2. Absorption of energy at a wide range of N_{res} leads to gradual increase in energy absorbed with increasing peak intensity as compared to the 100 fs case where there is a sharp threshold, marked by a transition to the $N_{res}=1$ state.

Another feature of Fig. 2 is the variation in the saturation value of energy absorbed for varying pulse duration. This is depicted explicitly in Fig. 7 where we plot the total energy absorbed per cluster electron versus pulse duration for an argon cluster and peak laser intensity of 1×10^{16} W/cm^2. We note that at this peak intensity the energy absorption curves (Fig. 2) for argon for all pulse durations have reached the saturation value. Figure 7 shows that the saturation value of

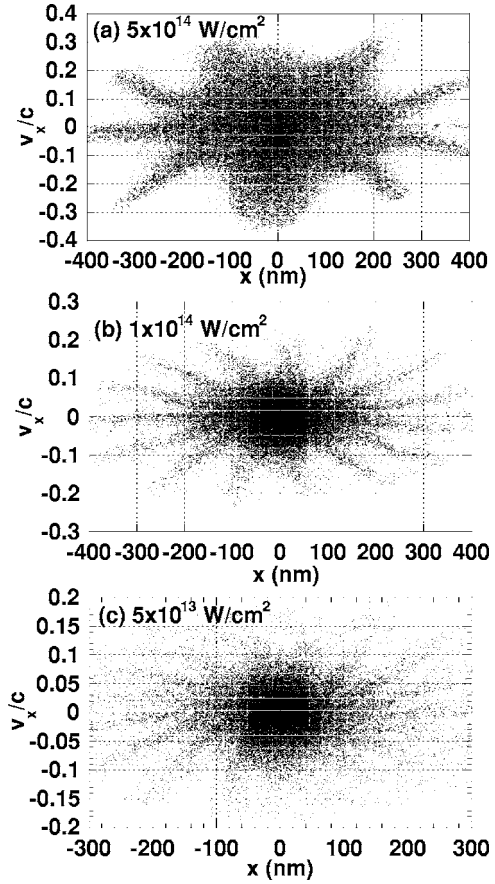

FIG. 6. Phase space (x-v_x) for electrons near the x-axis for argon cluster for 1 ps FWHM and peak intensity of (a) 5×10^{14} W/cm^2, (b) 1×10^{14} W/cm^2, and (c) 5×10^{13} W/cm^2 at $t=1720$ fs. The plots show that $N_{res}=9$, 15, and 19 for (a), (b), and (c), respectively.

absorbed energy increases with pulse duration till about 500 fs but decreases for the much longer pulse length of 1 ps. The cluster does not disintegrate fully for the shortest pulse lengths, and can thus absorb more energy as the pulse length is increased. However, as the pulse length is increased to 1 ps the cluster expands and disintegrates earlier in the pulse. Thus, most of the pulse energy is unabsorbed as it passes through the tenuous plasma formed by the cluster explosion. Our simulations thus indicate a maximum saturation value for 500 fs pulse length (though this observation is limited by the small number of data points on this plot). The trend in Fig. 7 is similar to the trend seen in experiments on studies of energy absorbed by exploding Argon clusters (Fig. 3 in the paper by Zweiback *et al.* [27]). The experimental study by Zweiback [27] found the energy absorption to peak between pulse lengths 200 fs to 300 fs for Argon clusters varying in diameter from 22 nm–33 nm. The peak intensity was 1.9×10^{17} W/cm^2 for a 50 fs pulse. Our simulations are limited in their consideration of a single cluster in a laser field while in an experiment absorption of laser energy in a cluster jet would be affected by additional factors such as the size distribution of clusters, number density and spatial distribution of clusters and propagation of the laser pulse. However, incorporation of these additional factors should not affect the qualitative trend that we observe in the energy

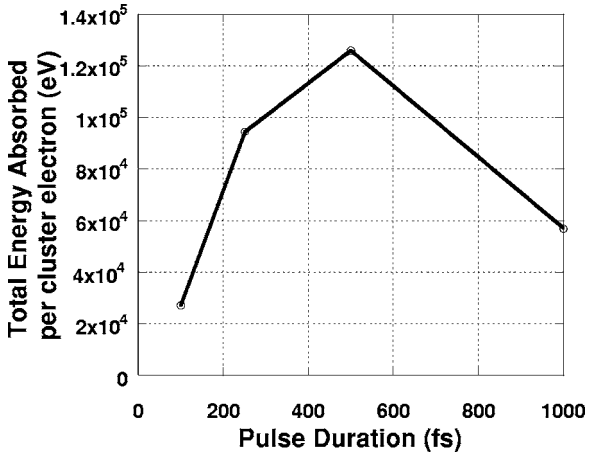

FIG. 7. Total energy absorbed per cluster electron (eV) versus pulse length (fs) for argon cluster and peak laser intensity of 1×10^{16} W/cm^2. This peak intensity is much beyond the strong heating threshold for all the pulse durations under consideration and thus the plotted energy absorbed represents the saturation value for the corresponding pulse length. The trend in the energy absorbed as seen here is similar to that observed in Fig. 3 of the journal article by Zweiback *et al.* [27].

absorbed by clusters, and the experimental results [27] lends qualitative confirmation to our model.

Finally in Fig. 2 we note that the intensity threshold for circularly polarized laser pulse is higher than that for the linearly polarized pulse. Figure 2 shows that the intensity threshold for circular polarization is just below 1×10^{16} W/cm^2 while the corresponding point for the linear polarization case is 5×10^{15} W/cm^2. For the same peak laser intensity, the peak electric field in any one direction for circularly polarized case is $1/\sqrt{2}$ times the linearly polarized field in the polarization direction. Thus for the circularly polarized pulse the threshold peak laser intensity needs to be twice that for linearly polarized case for the transit time resonance of $N_{res}=1$.

IV. ELECTRON AND ION ENERGY DISTRIBUTION FUNCTIONS

Figure 8 plots (a) the electron kinetic energy spectra, $F_e(E,t)$, and (b) the ion kinetic energy spectra, $F_i(E,t)$ for an irradiated argon cluster. The product $(F_{e,i}dE)$ represents the fraction of electrons (ions) in the interval dE at a given kinetic energy E. The three spectra labeled (a–c) in each plot correspond to laser pulses of equal energy for the following pulse width and peak intensity combinations: (a) 100 fs, 1×10^{16} W/cm^2; (b) 250 fs, 4×10^{15} W/cm^2; (c) 1000 fs, 1×10^{15} W/cm^2. Each of these cases considered is above the threshold for strong heating. A quasimonoenergetic peak characterizes the energy distribution of the emerging ions. As electrons are extracted from the cluster by the laser electric field they form a halo of energetic electrons around the cluster. The ions gain energy as they are pulled out by this space charge around the cluster. Initially this leads to an ion energy distribution that is monotonic in energy and radial distance

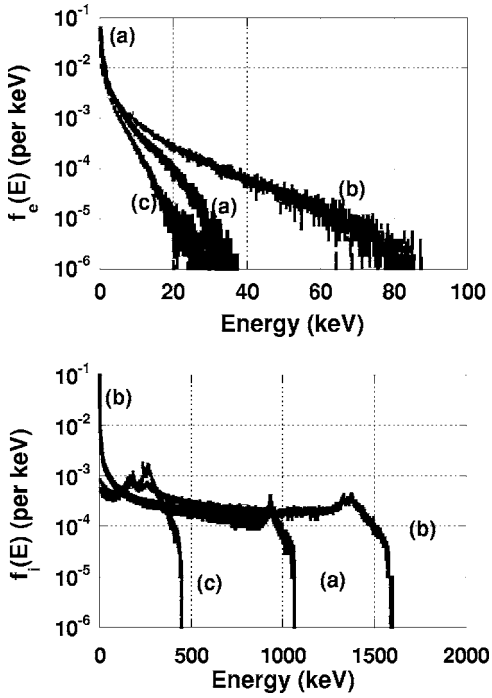

FIG. 8. Electron (a) and ion (b) kinetic energy distribution functions for (a) 100 fs, 1×10^{16} W/cm^2, (b) 250 fs, 4×10^{15} W/cm^2, and (c) 1 ps, 1×10^{15} W/cm^2. A quasimonoenergetic peak of ions dominates the ion distribution function. The energy at which this peak occurs is pulse duration dependent. For both electron and ions, the distribution functions show an increase in energy as the pulse length is increased from 100 fs to 250 fs, but in either case the energy falls down as the pulse length is further increased to 1 ps.

with the highest energy ions also being at the largest radial distance from the center of the cluster. As the ions and electrons expand, the electrostatic potential changes with time. This results in ions that have been accelerated later gaining more energy and over taking the ions accelerated earlier. The beamlike distribution is associated with this overtaking process that leads to an increase in the population of ions at energy slightly below the maximum energy.

Both electron and ion kinetic energy distributions show an increase in the energy as the pulse width is increased from 100 fs to 250 fs and then the energy falls as the pulse width is further increased to 1 ps. This trend follows that of the average energy absorbed in the saturated regime depicted in Fig. 3. The effect is more dramatic for ions with the peak ion energy varying from about 800 keV for laser FWHM of 100 fs (a) to 1400 keV for 250 fs FWHM (b) and finally falling to 250 keV for 1000 fs (c). To explain this we note that for pulse duration of 100 fs, the cluster does not disintegrate completely by the time the pulse has passed over it. Thus if the pulse duration is increased from 100 fs the cluster can absorb heat for a longer period of time before it disintegrates. This leads to higher absorption of energy by the cluster electrons and the corresponding higher ion energies. However, as the pulse duration is increased further the cluster starts disintegrating earlier in the pulse. Once the cluster has disintegrated and the electrons respond as if they were free (that is, the self-field of the cluster is unimportant) heating stops. This leads to the fall in the peak electron and ion energies as observed for the 1 ps case. This also explains the higher saturation value of the total energy absorbed by the cluster for the 250 fs pulse duration as compared to the 100 fs and 1 ps pulses.

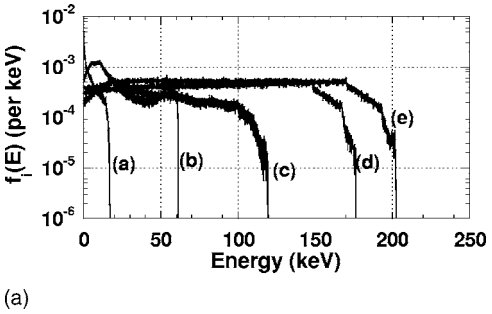

(a)

FIG. 9. Ion kinetic energy distribution functions under periodic boundary conditions for Deuterium ions of initial diameter 38 nm irradiated with laser pulses of 100 fs duration and peak intensities of (a) 1×10^{15} W/cm^2, (b) 3×10^{15} W/cm^2, (c) 1×10^{16} W/cm^2, (d) 5×10^{16} W/cm^2, and (e) 1×10^{17} W/cm^2.

As a cluster expands it eventually encounters particles from neighboring clusters. The greater the number density of clusters, the sooner this would happen. Generally when the expanding clusters encounter one another the result is that the accelerating potential resulting due to the expanding electrons is driven to zero and evolution of the distribution functions ceases. Using periodic boundary conditions in the simulations allows for such intercluster ion and electron interaction to take place. Figure 9 plots the ion energy distribution functions, $f_i(E,t)$ versus energy for a 38 nm deuterium cluster. The curves labeled (a)–(e) are obtained using periodic boundary conditions peak laser intensities of 1×10^{15} W/cm^2, 3×10^{15} W/cm^2, 1×10^{16} W/cm^2, 5×10^{16} W/cm^2, and 1×10^{17} W/cm^2, respectively. As in the case of argon clusters, we see an ion distribution function dominated by high-energy ions for intensities above the threshold for strong heating at 3×10^{15} W/cm^2. The spectrum for the below-threshold peak laser intensity of 1×10^{15} W/cm^2, marked as (a), does not have this character. The space charge field for such low laser intensities is not enough to accelerate a large number of ions to the boundary of the electron cloud surrounding the cluster. For intensities much higher than the threshold intensity the distribution function actually increases with increasing energy, reaches a maximum and then finally falls off. Also, the maximum ion energy is seen to increase monotonically with the peak laser intensity. In the following section we show how this pronounced dependence of the ion energy spectrum on the peak laser intensity would impact the fusion yields for laser-irradiated clusters.

V. FUSION NEUTRON YIELD

Energetic ions from exploding deuterium clusters can undergo thermonuclear fusion producing neutrons as represented by the reaction

$$D + D \xrightarrow[50\%]{} He^3(0.82\ MeV) + n(2.45\ MeV). \quad (4)$$

To calculate the rate of fusion reactions we assume that the ions at all energies are distributed uniformly in space. This is a reasonable assumption for periodic boundary conditions towards the end of the pulse when the energetic ions have expanded to beyond the simulation boundary. There is also the possibility of neutron production via two-step process such as

$$D + D \xrightarrow[50\%]{} T + p,$$

$$D + T \xrightarrow[50\%]{} He^4 + n, \quad (5)$$

but for the parameter ranges under consideration the total yield of products from the first reaction in Eq. (5) is not large enough to necessitate the consideration of follow-up reaction. Hence we only consider Eq. (4) here for calculating neutron yield. The number of fusion reaction per second per unit volume is then given as

$$R(t) = \frac{1}{2} {n_{av}}^2 \int dE \int dE' f_i(E,t) f_i(E',t) \langle \sigma(E_{rel}) |\mathbf{v} - \mathbf{v}'| \rangle_\theta, \quad (6)$$

where n_{av} is the average density of ions over the simulation region, $f_i(E,t)$ is the kinetic energy distribution of ions given by, σ is the reaction cross section, and $\mathbf{v}$ is the ion velocity such that $m_i|\mathbf{v}|^2 = 2E$, m_i being the ion mass. The reaction cross section σ is expressed as a function of the relative energy of the interacting ions, $E_{rel} = m_i|\mathbf{v} - \mathbf{v}'|^2/2$ where $\mathbf{v}$ and $\mathbf{v}'$ are the velocities of the interacting ions. The angled brackets denote an averaging over all possible angles θ, assuming that the ion distribution is isotropic. Equation (7) below gives the reaction cross section [28] (in cm^2)

$$\sigma(E_{rel}) = \frac{A_5 + [\{A_4 - A_3(E_{rel})\} + 1]^{-1} A_2}{(E_{rel})[\exp\{A_4 (E_{rel})^{-1/2}\} - 1]} \times 10^{-24}, \quad (7)$$

where (E_{rel}) is in keV. The Duane coefficients A_j have the values $A_1 = 47.88$, $A_2 = 482$, $A_3 = 3.08 \times 10^{-4}$, $A_4 = 1.177$, and $A_5 = 0$ for the particular reaction in Eq. (4).

In order to calculate the yield of fusion neutrons we consider a cylindrical volume, $V = (2\pi w_0)(2z_r)$ where w_0 is the spot size of the laser beam and z_r is the Rayleigh length associated with that spot size. We assume that the interaction time for ions is limited by the average time required by the higher energy ion to exit this volume. The total neutron yield can then be calculated as

$$NY = \frac{1}{2} {n_{av}}^2 V D_{avg} \int dE \int dE' f_i(E,t) f_i(E',t) \times \langle \sigma(E_{rel}) |\mathbf{v} - \mathbf{v}'| \rangle_\theta \frac{1}{\max(|\mathbf{v}|, |\mathbf{v}'|)}, \quad (8)$$

where D_{avg} is the average distance from the center to the edge of the volume under consideration.

Figure 10 plots reaction rate per unit volume at $t = 300$ fs (solid) and total neutron yield (dotted) for fusion of energetic ions from exploding laser-irradiated deuterium clusters with pulse peak intensities ranging from 1×10^{15} W/cm^2 to 1×10^{17} W/cm^2. The threshold intensity for this set of runs was at 3×10^{15} W/cm^2. The plot shows a sharp rise in the reaction rate as the intensity crosses the nonlinear resonance threshold. This is due to the increase in the number of high-energy ions as the intensity crosses the threshold. For intensities much above the threshold, the fusion rate and neutron yield both saturate as the cluster disintegrates earlier in the pulse.

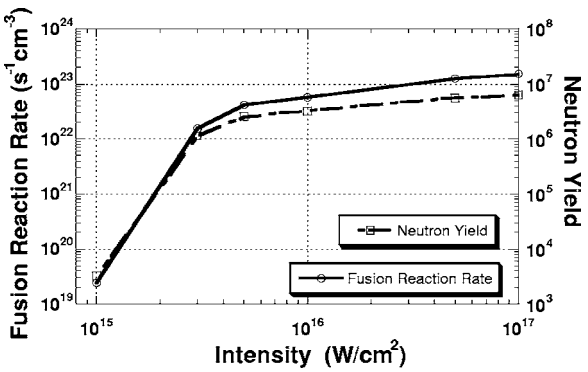

FIG. 10. Fusion reaction rate per unit volume (left vertical axis) and total neutron yield (right vertical axis) as a function of peak laser intensity for deuterium clusters with $D_0 = 38$ nm.

It should be noted that in actual experiments effects such size distribution of clusters, absorption and self-focusing of the pulse, and spatial distribution of energetic ions would play a significant role in determining the total neutron yield. Thus the neutron yield in an experiment might be different from that based on the fusion reaction rate calculated here.

VI. CONCLUSIONS

We describe the effect of laser pulse width on resonant heating of laser-irradiated clusters. The clusters absorb heat via a nonlinear resonance mechanism where electrons are first accelerated out from the cluster and then driven back into it by the combined effects of the laser field and the electrostatic field produced by the laser-driven charge separation. The energetic electrons then pass through the cluster and emerge on the other side. If they emerge in phase with the laser field, there is resonant heating, and the cluster quickly absorbs energy. The onset of this "transit time" resonance depends on the ratio of laser intensity to cluster size for a given pulse duration. Our simulations of argon and deuterium clusters show that as the pulse duration is increased the cluster absorbs energy at higher order resonances with the electron transit time equaling more than one laser period. This increase in the order of the resonance leads to the lowering of the intensity threshold for strong heating. As the pulse length is increased further our simulations how that the threshold becomes less dramatic and almost disappears for 1 ps pulse length. This is because at increased pulse lengths, even for low peak intensities the cluster can absorb significant energy due to longer times in high order resonant states. The calculation for predicting intensity threshold for a

given cluster diameter as derived in Ref. [17] has been generalized to take the higher order resonances into account. Our generalized formulation predicts intensity thresholds that are inversely proportional to the square of the order of resonance during strong heating. However, the predicted threshold intensities increasingly deviate from the values obtained from simulations as the pulse width is increased to 1000 fs. This is due to cluster expansion earlier in the pulse for longer pulse widths, an effect that was not taken into account for calculating the predicted intensity thresholds.

Our results indicate a strong pulse duration dependence of the kinetic energy distribution of the cluster ions and electrons with the maximum ion energy going up from 800 keV to 1.4 MeV as the pulse width is increased from 100 fs to 250 fs, but then falling off to 250 keV as the pulse width is increased further to 1000 fs. The pulse energy was kept constant for this set of runs. This trend in the maximum energy of ions mimics the trend in saturation value of energy absorbed the cluster for different pulse lengths and is consistent with the experimental results by Zweiback *et al.* of laser pulse energy absorption by argon clusters for varying pulse lengths [27]. This is of consequence for possible applications in laser-based accelerators and for fusion neutron production from clusters.

We have investigated the fusion reaction rate and neutron yield for deuterium clusters for a 100 fs FWHM pulse of peak intensities ranging from 10^{15}–10^{17} W/cm^2. We find that there is a dramatic increase in the reaction rate and neutron yield as the intensity crosses the threshold for strong heating at 3×10^{15} W/cm^2. The reaction rate saturates beyond the peak intensity of 5×10^{15} W/cm^2 as the intensity is increased to 1×10^{17} W/cm^2.

[1] O. F. Hagena and W. Obert, J. Chem. Phys. **56**, 1793 (1972).
[2] T. Ditmire, R. A. Smith, J. W. G. Tisch, and M. H. R. Hutchinson, Phys. Rev. Lett. **78**, 3121 (1997).
[3] K. Y. Kim, I. Alexeev, V. Kumarappan *et al.*, Phys. Plasmas **11**(5), 2882 (2004).
[4] Y. L. Shao, T. Ditmire, J. W. G. Tisch, E. Springate, J. P. Marangos, and M. H. R. Hutchinson, Phys. Rev. Lett. **77**, 3343 (1996); V. Kumarappan, M. Krishnamurthy, and D. Mathur, *ibid.* **87**, 085005 (2001).
[5] T. Ditmire, J. Zweiback, V. P. Yanovsky *et al.*, Nature (London) **398**, 489 (1999).
[6] K. W. Madison, P. K. Patel, M. Allen *et al.*, J. Opt. Soc. Am. B **20**, 113 (2003).
[7] T. D. Donnelly, T. Ditmire, K. Neuman, M. D. Perry, and R. W. Falcone, Phys. Rev. Lett. **76**, 2472 (1996).
[8] I. Alexeev, T. M. Antonsen, K. Y. Kim, and H. M. Milchberg, Phys. Rev. Lett. **90**, 103402 (2003).
[9] T. Ditmire, R. A. Smith, and M. H. R. Hutchinson, Opt. Lett. **23**, 322 (1998); V. Kumarappan, K. Y. Kim, and H. M. Milchberg, Phys. Rev. Lett. **94**, 205004 (2005).
[10] V. Kumarappan, M. Krishnamurthy, D. Mathur, and L. C. Tribedi, Phys. Rev. A **63**, 023203 (2001); E. Springate, N. Hay, J. W. G. Tisch, M. B. Mason, T. Ditmire, M. H. R. Hutchinson, and J. P. Marangos, *ibid.* **61**, 063201 (2000); T. Ditmire, R. A. Smith, R. S. Marjoribanks *et al.*, Appl. Phys. Lett. **71**, 166 (1997).
[11] K. W. Madison, P. K. Patel, D. Price *et al.*, Phys. Plasmas **11**, 270 (2004).
[12] K. W. Madison, P. K. Patel, M. Allen, D. Price, R. Fitzpatrick, and T. Ditmire, Phys. Rev. A **70**, 053201 (2004).
[13] E. Parra, I. Alexeev, J. Fan, K. Kim, S. J. McNaught, and H. M. Milchberg, Phys. Rev. E **62**, R5931 (2000).
[14] B. N. Breizman, A. V. Arefiev, and M. V. Fomyts'kyi, Phys. Plasmas **12**, 056706 (2005).
[15] F. Greschik, L. Arndt, and H. J. Kull, Europhys. Lett. **72**, 376 (2005).
[16] H. M. Milchberg, S. J. McNaught, and E. Parra, Phys. Rev. E **64**, 056402 (2001).
[17] T. Taguchi, T. M. Antonsen, and H. M. Milchberg, Phys. Rev. Lett. **92**, 205003 (2004).
[18] T. M. Antonsen, T. Taguchi, A. Gupta *et al.*, Phys. Plasmas **12**, 056703 (2005).
[19] Y. Kishimoto, T. Masaki, and T. Tajima, Phys. Plasmas **9**, 589 (2002).
[20] J. Zweiback, T. Ditmire, and M. D. Perry, Opt. Express **6**, 236 (2000).
[21] M. Schnurer, S. Ter-Avetisyan, H. Stiel *et al.*, Eur. Phys. J. D **14**, 331 (2001).
[22] K. Ishikawa and T. Blenski, Phys. Rev. A **62**, 063204 (2000); G. M. Petrov, J. Davis, A. L. Velikovich, P. Kepple, A. Dasgupta, R. W. Clark, A. B. Borisov, K. Boyer, and C. K. Rhodes, Phys. Rev. E **71**, 036411 (2005); G. M. Petrov, J. Davis, A. L. Velikovich *et al.*, Phys. Plasmas **12**, 063103 (2005); M. Eloy, R. Azambuja, J. T. Mendonca *et al.*,Phys. Scr. **T89**, 60 (2001).
[23] T. Ditmire, T. Donnelly, A. M. Rubenchik, R. W. Falcone, and M. D. Perry, Phys. Rev. A **53**, 3379 (1996).
[24] F. Greschik and H. Kull, Laser Part. Beams **22**, 137 (2004).
[25] F. Brunel, Phys. Rev. Lett. **59**, 52 (1987).
[26] J. Zweiback, T. E. Cowan, J. H. Hartley *et al.*, Phys. Plasmas **9**, 3108 (2002); J. Zweiback, R. A. Smith, T. E. Cowan, G. Hays, K. B. Wharton, V. P. Yanovsky, and T. Ditmire, Phys. Rev. Lett. **84**, 2634 (2000).
[27] J. Zweiback, T. Ditmire, and M. D. Perry, Phys. Rev. A **59**(5), R3166 (1999).
[28] G. H. Miley, H. Towner, and N. Ivich, 1974; B. H. Duane, 1972.